

## Penning detachment of $H^-$ by impact of excited He and Li atoms

F. Martín\* and R. S. Berry

Department of Chemistry and The James Franck Institute, The University of Chicago, 5735 South Ellis Avenue, Chicago, Illinois 60637-1403

(Received 10 June 1996; revised manuscript received 5 September 1996)

We present calculations of electron detachment from slow  $H^-$  ions with excited He and Li atoms. The theoretical method is based on a close-coupling expansion of the electronic wave function and makes use of a discretization technique to describe the continuum. The calculated cross sections for these processes typically vary from  $\approx 10^{-13} \text{ cm}^2$  at 50 meV to  $10^{-14} \text{ cm}^2$  at 20 eV and are the result of (i) the attractive nature of the interatomic potential and (ii) the Stark mixing induced by the ion on the excited neutral atom. [S1050-2947(97)03702-5]

PACS number(s): 34.50.Fa

### I. INTRODUCTION

Among the many processes that atomic or molecular collisions may induce, one has gone almost unnoticed, despite both the attention paid to closely related processes and the likelihood that its associated cross sections are large. This is the process in which a negative ion  $A^-$  collides with an electronically excited energy donor  $N^*$  and the energy of excitation passes from the donor to the negative ion and sets the excess electron free, leaving as final products  $A+N+e^-$ . This is analogous to Penning ionization, in which the energy donor  $N^*$  collides with a neutral atom whose ionization energy is less than the excitation contained in  $N^*$ , so that the final products are  $A^++N+e^-$ . On this basis, we shall call the detachment process described here ‘‘Penning detachment.’’

One investigation, by Blaney and Berry [1], produced order-of-magnitude estimates of some cross sections for Penning detachment. These indicated that the process is likely to have a high probability; typical estimates from that work were cross sections of order  $10^{-14} \text{ cm}^2$ . An experimental study by Fehsenfeld *et al.* [2] reported the occurrence of detachment of electrons from  $O^-$  by collision with excited oxygen molecules. Detachment of electrons from  $Cl^-$  ions by collision with optically excited sodium atoms was the object of a study reported briefly by Doweck *et al.* [3]. These three seem to be the only reports in the literature directly related to Penning detachment.

Here we report the results of fairly robust calculations of the cross sections for Penning detachment of electrons from  $H^-$  by collision with  $He^*$  and with  $Li^*$ . These calculations are meant to be complementary to the experiments reported by Darveau *et al.* [4] demonstrating Penning detachment of electrons from  $O^-$  by collision with optically excited calcium atoms  $Ca(4s4p^1P)$ . The calculations are not yet developed enough to treat precisely the problem examined in the experiments, but they do address processes that are accessible experimentally and they illustrate some general proper-

ties of the process that the experiments of Darveau *et al.* can reveal.

The next section treats the methods used to carry out the calculations. Section III describes the calculations themselves and Sec. IV presents the cross sections. Section V is a discussion of these results and their implications. Atomic units are used throughout unless stated otherwise.

### II. GENERAL THEORY

#### A. Close coupling

We treat the problem semiclassically in this sense: the nuclei follow classical trajectories in the field induced by the effective interatomic potential, whereas the electrons are described quantum mechanically. On any given nuclear trajectory, the electronic wave function is the solution of the Schrödinger equation

$$i\frac{d}{dt}\Psi(t) = \mathcal{H}_{el}\Psi(t), \quad (1)$$

where  $\mathcal{H}_{el}$  is the molecular Born-Oppenheimer Hamiltonian that depends parametrically on time through the internuclear distance  $R(t)$ ,  $\Psi(t)$  is the electronic wave function, and  $t$  is the time coordinate of the collision event. The initial state of the system,  $A^-+N^*$ , is embedded in the electronic continuum of the molecular negative ion  $AN^-$  formed during the collision. With this picture in mind, we define a basis of adiabatic states as follows. Bound electronic states for  $t = -\infty$  are formally the solutions of

$$(Q\mathcal{H}_{el}Q - E_i)\psi_i = 0 \quad (2)$$

and (unbound) electronic continuum states are the solutions of

$$(P_l\mathcal{H}_{el}P_l - E)\psi_{E,l} = 0, \quad (3)$$

where  $l$  is the angular momentum of the ejected electron and  $P_l$  and  $Q$  are projection operators that satisfy the exclusionary conditions

$$P_l P_{l'} = \delta_{ll'}, \quad (4)$$

\*Permanent address: Departamento de Química C-9, Universidad Autónoma de Madrid, 28049 Madrid, Spain.

$$P = \sum_l P_l, \quad (5)$$

$$PQ = 0, \quad (6)$$

$$P + Q = 1 \quad (7)$$

for all  $R$ . Notice that  $\mathcal{H}_{\text{el}}$  is not completely diagonal in the  $\{\psi_i, \psi_{E,l}\}$  basis because, in general,  $\langle \psi_i | Q \mathcal{H}_{\text{el}} P_l | \psi_{E,l} \rangle$  and  $\langle \psi_{E,l} | P_l \mathcal{H}_{\text{el}} P_{l'} | \psi_{E,l'} \rangle$  are different from zero. Therefore, the  $\{\psi_i, \psi_{E,l}\}$  basis is adiabatic in the sense that Eqs. (2) and (3) are fulfilled for all  $R$ . We expand the electronic wave function  $\Psi(t)$  in this basis

$$\begin{aligned} \Psi(t) = & \sum_i c_i(t) \exp\left(-i \int_{-\infty}^t E_i dt'\right) \psi_i \\ & + \sum_l \int dE c_{E,l}(t) \exp\left(-i \int_{-\infty}^t E dt'\right) \psi_{E,l} \end{aligned} \quad (8)$$

and use the single-state initial condition

$$c_i(-\infty) = \delta_{i0}, \quad (9)$$

$$c_{E,l}(-\infty) = 0, \quad (10)$$

where  $\psi_0$  represents the initial state. Substitution of Eq. (8) into Eq. (1) leads to the system of differential equations

$$\begin{aligned} i \frac{d}{dt} c_i(t) = & \sum_l \int dE \exp\left(i \int_{-\infty}^t (E_i - E) dt'\right) \\ & \times \langle \psi_i | Q \mathcal{H}_{\text{el}} P_l | \psi_{E,l} \rangle c_{E,l}(t), \end{aligned} \quad (11)$$

$$\begin{aligned} i \frac{d}{dt} c_{E,l}(t) = & \sum_i c_i(t) \exp\left(i \int_{-\infty}^t (E - E_i) dt'\right) \\ & \times \langle \psi_{E,l} | P_l \mathcal{H}_{\text{el}} Q | \psi_i \rangle + \sum_{l' \neq l} \int dE' c_{E',l'}(t) \\ & \times \exp\left(i \int_{-\infty}^t (E - E') dt'\right) \\ & \times \langle \psi_{E,l} | P_l \mathcal{H}_{\text{el}} P_{l'} | \psi_{E',l'} \rangle. \end{aligned} \quad (12)$$

In Eq. (12) we have neglected all dynamical couplings corresponding to the breakdown of the Born-Oppenheimer approximation. For the collision velocities considered in this work this is a very good approximation: explicit calculations including those couplings at 1 eV are practically indistinguishable from those excluding them. This can be easily understood because the dynamical couplings are proportional to the collision velocity, which in the present work is of the order of  $10^{-3}$  a.u. In Eqs. (11) and (12), the couplings  $\langle \psi_i | Q \mathcal{H}_{\text{el}} P_l | \psi_{E,l} \rangle$  are responsible for bound-continuum transitions and therefore for Penning detachment. The couplings  $\langle \psi_{E,l} | P_l \mathcal{H}_{\text{el}} P_{l'} | \psi_{E',l'} \rangle$  represent continuum-continuum transitions and therefore they are responsible for a redistribution of the population within the continuum. The total ionization cross section is given by

$$\sigma_{\text{ion}} = 2\pi \int_0^\infty b P(b) db, \quad (13)$$

where

$$P(b) = \lim_{t \rightarrow \infty} P(b, t) = \lim_{t \rightarrow \infty} \sum_l \int dE |c_{E,l}(\infty)|^2 \quad (14)$$

and  $b$  is the impact parameter.

## B. Local approximation

We show here that the usual local approximation, which assumes an exponential decay of the resonant state formed in the collision (see [5,6] and references therein), can be derived from the system of differential equations (11) and (12). Our results of Sec. III show that the local approximation is very accurate in the cases investigated here and can be used as an alternative to the close-coupling calculations.

First, we assume that the entrance channel is well separated in energy from the remaining  $Q$  states (isolated resonance approximation). Then, since there is no direct coupling in Eqs. (11) and (12) among the  $\psi_i$  states belonging to the  $Q$  subspace, we can neglect all  $Q$  states except the one that corresponds to the entrance channel  $\psi_0$ .

Second, from Eqs. (11) and (12) one can write

$$\begin{aligned} \frac{d}{dt} P(b, t) = & \sum_l \int dE \frac{d}{dt} |c_{E,l}(t)|^2 \\ = & - \frac{d}{dt} |c_0(t)|^2 \\ = & \text{Im} \left[ \sum_l c_0(t) \int dE c_{E,l}^* \exp\left(i \int_{-\infty}^t (E - E_0) dt'\right) \right. \\ & \left. \times \langle \psi_{E,l} | P_l \mathcal{H}_{\text{el}} Q | \psi_0 \rangle \right], \end{aligned} \quad (15)$$

which shows that the variation with time of the total ionization probability does not depend explicitly on the  $\langle \psi_{E,l} | P_l \mathcal{H}_{\text{el}} P_{l'} | \psi_{E',l'} \rangle$  couplings. Equation (15) is identical to the one that would be obtained if all those continuum-continuum couplings were zero. Therefore, if one is not interested in the actual population for each value of  $l$  and  $E$ , the neglect of such couplings is a reasonable approximation.

Using these two approximations, we can write, from Eq. (12),

$$\begin{aligned} c_{E,l}(t) = & -i \int_{-\infty}^t dt' c_0(t') \exp\left(i \int_{-\infty}^{t'} (E - E_0) dt''\right) \\ & \times \langle \psi_{E,l} | P_l \mathcal{H}_{\text{el}} Q | \psi_0 \rangle. \end{aligned} \quad (16)$$

Substitution into Eq. (11) leads to

$$\begin{aligned} \frac{d}{dt} c_0(t) = & - \sum_l \int dE \langle \psi_0 | Q \mathcal{H}_{\text{el}} P_l | \psi_{E,l} \rangle \\ & \times \int_{-\infty}^t dt' c_0(t') \exp\left(i \int_{t'}^t (E_0 - E) dt''\right) \\ & \times \langle \psi_{E,l} | P_l \mathcal{H}_{\text{el}} Q | \psi_0 \rangle. \end{aligned} \quad (17)$$

Now, let us call  $\Delta E$  an energy interval such that  $\langle \psi_0 | Q \mathcal{H}_{el} P_l | \psi_{E,l} \rangle$  barely changes in the interval  $I_{E_0} = [E_0 - \Delta E, E_0 + \Delta E]$ . If the collision velocity  $\mathbf{v}(t) = \mathbf{v}_0 - \mu^{-1} \int_{-\infty}^t \nabla V dt'$  (where  $V$  is the interatomic potential,  $\mu$  the reduced mass of the nuclei, and  $\mathbf{v}_0$  the initial velocity in a.u.) is small enough such that  $|\mathbf{v}| < \Delta E$  for all  $t$ , the integral in Eq. (17) is almost zero outside  $I_{E_0}$  due to the strongly oscillatory behavior of the exponential. Then, Eq. (17) leads to

$$\frac{d}{dt} c_0(t) \approx -\pi c_0(t) \sum_l |\langle \psi_0 | Q \mathcal{H}_{el} P_l | \psi_{E=E_0,l} \rangle|^2, \quad (18)$$

so that the total ionization probability for a given trajectory can be written

$$P(b) = 1 - \exp\left(-\int_{-\infty}^{\infty} \Gamma(t) dt\right), \quad (19)$$

where

$$\Gamma(t) = 2\pi \sum_l |\langle \psi_0 | Q \mathcal{H}_{el} P_l | \psi_{E=E_0,l} \rangle|^2. \quad (20)$$

Equation (19) can also be written

$$P(b) = 1 - \exp\left(-2 \int_{R_0}^{\infty} \Gamma(R)/v(R) dR\right), \quad (21)$$

where  $v(R)$  is the radial velocity of the nuclei

$$v(R) = \frac{1}{v_0 \sqrt{1 - \frac{2V(R) - b^2}{\mu v_0^2 R^2}}} \quad (22)$$

and  $R_0$  is the classical turning point.

### C. Adiabatic states

Penning detachment is essentially a two-electron process in which the energy of the excited electron of the neutral atom is transferred to the loosely bound electron of the negative ion. In the present model used here, all other electrons remain passive during the collision. Therefore, the dynamics of the Penning detachment process can be studied using an effective two-electron Hamiltonian. This Hamiltonian can be written

$$\begin{aligned} \mathcal{H}_{el} = & -\frac{1}{2} \nabla_1^2 - \frac{1}{2} \nabla_2^2 + V_{A-}(1) + V_{A-}(2) \\ & + V_N(1) + V_N(2) + \frac{1}{r_{12}}, \end{aligned} \quad (23)$$

where  $V_{A-}$  ( $V_N$ ) is the potential that describes the interaction between an electron and the core of the negative ion (the neutral atom). In this work we have used the simple forms

$$V_{A-} = -\frac{Z_A}{r_A} (1 + \alpha_A r_A) e^{-2\alpha_A r_A}, \quad (24)$$

$$V_N = -\frac{1}{r_N} - \frac{(Z_N - 1)}{r_N} (1 + \alpha_N r_N) e^{-2\alpha_N r_N}, \quad (25)$$

which are widely used in the study of ion-atom collisions [7] as well as in atomic structure calculations [8]. Notice that both potentials have the correct asymptotic behavior

$$\lim_{r_A \rightarrow 0} V_{A-} = -\frac{Z_A}{r_A}, \quad (26)$$

$$\lim_{r_A \rightarrow \infty} V_{A-} = 0 \quad (27)$$

and

$$\lim_{r_N \rightarrow 0} V_N = -\frac{Z_N}{r_N}, \quad (28)$$

$$\lim_{r_N \rightarrow \infty} V_N = -\frac{1}{r_N}. \quad (29)$$

The  $Q$  states are obtained by diagonalizing  $Q \mathcal{H}_{el} Q$  in a basis of (properly antisymmetrized) two-electron configurations of the form  $\{\varphi_{1s_A^-} \varphi_{k_N}\}$ , where  $\varphi_{1s_A^-}$  is the lowest one-electron orbital of the anion

$$(-\frac{1}{2} \nabla^2 + V_{A-}) \varphi_{1s_A^-} = \epsilon_{1s_A} \varphi_{1s_A^-} \quad (30)$$

and the  $\varphi_{k_N}$  orbitals are the solutions of

$$(-\frac{1}{2} \nabla^2 + V_N) \varphi_{k_N} = \epsilon_{k_N} \varphi_{k_N}. \quad (31)$$

Two-electron configurations with both electrons in  $N$  are not included in the diagonalization procedure since their contribution to the Penning detachment process is expected to be small. The  $\varphi$  orbitals are written as linear superpositions of Gaussian-type orbitals (GTOs).

The  $P$  states are (properly antisymmetrized) two-electron configurations of the form  $\tilde{\psi}_{E,l} = \tilde{\varphi}_{\epsilon,l} \varphi_{v_N}$ , where  $\varphi_{v_N}$  is the valence orbital of the neutral atom and the  $\tilde{\varphi}_{\epsilon,l}$  functions are discretized continuum orbitals. The latter correspond to those solutions with energies lying above the ionization threshold and are obtained by diagonalizing Eq. (30) using an even-tempered sequence of GTOs for each  $l$  [9]. The eigenfunctions  $\tilde{\varphi}_{\epsilon,l}$  resulting from this diagonalization are related to the properly normalized continuum orbitals  $\varphi_{\epsilon,l}$  through the equation

$$\varphi_{\epsilon,l} \approx \rho^{1/2}(\epsilon) \tilde{\varphi}_{\epsilon,l}, \quad (32)$$

where  $\rho$  is the density of continuum states. This quantity has been evaluated as in Ref. [9].

The use of a discretized basis of continuum states implies that all energy integrals  $\int dE$  in Eqs. (11) and (12) must be replaced by quadratures  $\sum_i \Delta \epsilon_i$ . The couplings

$$\langle \psi_{E_n,l} | P_l \mathcal{H}_{el} Q | \psi_0 \rangle \approx \rho^{1/2}(E_n) \langle \tilde{\psi}_{E_n,l} | P_l \mathcal{H}_{el} Q | \psi_0 \rangle \quad (33)$$

and

$$\langle \psi_{E_n, l} | P_l \mathcal{H}_{\text{el}} P_l' | \psi_{E_{n'}, l'} \rangle \approx \rho^{1/2}(E_n) \rho^{1/2}(E_{n'})$$

$$\times \langle \psi_{E_n, l} | P_l \mathcal{H}_{\text{el}} P_l' | \psi_{E_{n'}, l'} \rangle \quad (34)$$

are only known for the energies  $E_n$  resulting from the diagonalization of Eq. (30) in the GTO basis. In the present problem, the energy spacing required to achieve convergence in the quadrature is much smaller than the energy spacing provided by such a diagonalization. However, since the couplings defined in Eqs. (33) and (34) vary smoothly with  $E$ , it is possible to obtain their values for any desired energy by simply interpolating the corresponding histograms for each  $R$ . Finally, we have verified that orthogonality between  $P$  and  $Q$  subspaces is well satisfied for  $R > 2$  a.u.

### III. CALCULATIONS

#### A. One-electron orbitals

The value of  $\alpha_{\text{H}^-}$  used in  $V_{\text{H}^-}$  [Eq. (24)] is  $\alpha_{\text{H}^-} = 0.6973$ , which provides a ground-state energy of  $-0.52703$  a.u. with our GTO basis. This is close to the actual value in  $\text{H}^-$  (the exact nonrelativistic ground-state energy computed by Pekeris [10] is  $-0.52775$  a.u.). This is the only bound state that we have found for all  $l$ , in agreement with the experimental observations. The values of  $\alpha_{\text{He}} = 1.6847$  and  $\alpha_{\text{Li}} = 1.6480$  have been chosen to reproduce simultaneously the ground and the excited states of the neutral atoms. In the case of Li, the lowest eigenfunction has to be excluded from the calculations since it corresponds to an unphysical virtual core state with three electrons in the  $1s$  shell.

To analyze the validity of the discretization technique for describing the one-electron continuum orbitals of  $\text{H}^-$ , we have compared the radial factors of the  $1s$  orbital of  $\text{H}^-$  with discretized continuum orbitals with energies  $\epsilon = 0.73$  and  $0.067$  a.u. These are the mean kinetic energies of the ejected electrons when  $\text{H}^-$  collides with  $\text{He}(1s2s, ^1S)$  and  $\text{Li}(1s^22p)$ , respectively. The exponential decay of the discretized continuum wave functions occurs far beyond the region where the  $1s$  orbital of  $\text{H}^-$  has significant amplitude, at a much larger distance in the low-energy, Li-initiated detachment than in the higher-energy, He-initiated example. The consequence of this examination is that we can be confident that the discretized wave functions yield reliable matrix elements between  $1s$  and continuum levels of  $\text{H}^-$ . The same holds for the direct and exchange terms of the two-electron matrix elements, although the exchange terms might be less accurate for the He example than for the case with Li.

#### B. Potential-energy curves and couplings

As explained in Sec. II C, the Schrödinger equation in  $Q$  space has been solved by diagonalizing  $Q\mathcal{H}_{\text{el}}Q$  in a basis of antisymmetrized two-electron configurations  $\{\varphi_{1s\text{H}^-} \varphi_{k_N}\}$ . The  $\varphi_{k_N}$  orbitals included in the present calculations are  $\varphi_{k_N} = 1s, 2s, 2p, 3s, 3p, 4s,$  and  $4p$  for He and  $\varphi_{k_N} = 2s, 2p, 3s, 3p, 3d, 4s, 4p,$  and  $4d$  for Li. In Figs. 1(a) and 1(b) we present the resulting eigenenergies as functions of the internuclear distance. These energies correspond to a spin

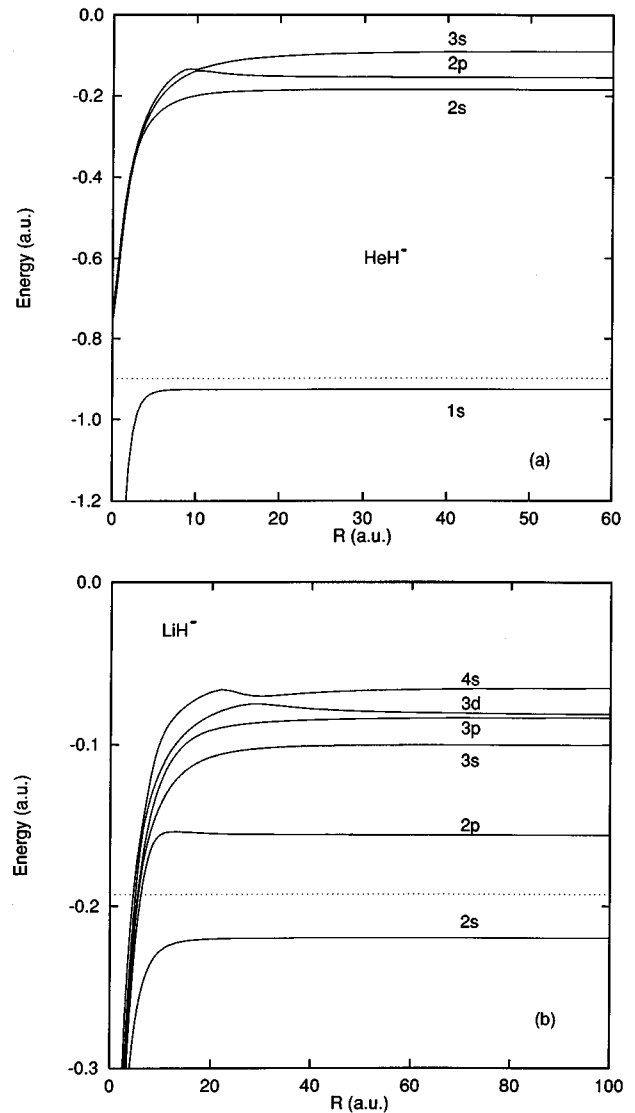


FIG. 1. Potential-energy curves for the (a)  $\text{HeH}^-$  and (b)  $\text{LiH}^-$  quasimolecules. The labels  $nl$  represent the asymptotic states  $\text{H}^- + \text{He}(1s nl)$  and  $\text{H}^- + \text{Li}(1s^2 nl)$ , respectively. The dotted lines show the position of the ionization thresholds  $\text{H} + \text{He}(1s^2) + e^-$  and  $\text{H} + \text{Li}(1s^2 2s) + e^-$ .

coupling  $S=0$ ; the corresponding values for  $S=1$  are very similar. Since the effective two-electron Hamiltonian of Eq. (23) includes two *atomic* model potentials, we expect our description of the  $\text{HeH}^-$  and  $\text{LiH}^-$  quasimolecules to break down when electron delocalization affects the atomic cores. This effect is negligible for  $R > 2$  a.u., so that the potential-energy curves shown in Fig. 1 should be reliable for  $R > 2$  a.u. In particular, the Stark mixing [11] within a given manifold (which is a fundamental effect to properly describe Penning detachment) is well described in the present calculations. Stark mixing is important at long distances, even well beyond 100 bohrs for the most extreme case we examined, of  $\text{H}^- + \text{Li}(1s^2 3d)$ . At these distances, delocalization effects on the atomic cores are completely negligible. As we will show in Sec. IV, the shape of the potential-energy curves shown in Fig. 1 is crucial to understand the variation of the Penning detachment cross sections with the collision energy.

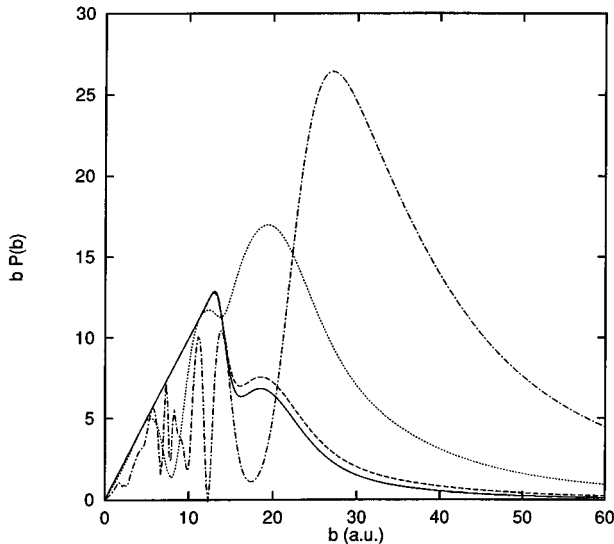


FIG. 2. Convergence of the Penning detachment transition probability for the  $H^- + Li(1s^2 2p)$  collision at 900 meV and spin coupling  $S=0$ . The close-coupling expansion includes the  $Q$  states shown in Fig. 1 and  $l=0$  and  $l=1$   $P$  states. The upper cutoff for  $P$  continuum states is placed 0.05 a.u. above the  $H^- + Li(1s^2 2p)$  resonance. The figure shows the variation of the transition probability times the impact parameter as a function of the impact parameter when the energy spacing between continuum states included in the close-coupling expansion (8) is 0.01 a.u. (dash-dotted line), 0.002 a.u. (dotted line), 0.0005 a.u. (dashed line), and 0.00025 a.u. (continuous line).

We have compared the  $\langle \psi_{E=E_0, l} | P_l \mathcal{H}_{el} Q | \psi_0 \rangle$  couplings obtained including and excluding exchange. We have found that exchange is important at rather large values of  $R$ . In general, exclusion of exchange leads to slightly smaller couplings, which would lead to smaller cross sections. For this reason, exchange has been included in all our *best* calculations.

### C. Convergence of the close-coupling calculations

We have solved the system of coupled equations (11) and (12) and checked the convergence with the size of the basis for the  $H^- + Li(1s^2 2p)$  collision at  $v_0=0.006$  a.u. and spin coupling  $S=0$ . As we will see in Sec. IV, in this particular example and for this energy, we can use straight-line trajectories to describe the nuclear motion. Although this may not be the case for all other systems and other collision energies, the consequences of this study will be of general validity.

We have found that the cross sections are practically insensitive to the number of  $Q$  states included in the close-coupling expansion. For example, results obtained by including only  $\phi_0$  (i.e., the state that asymptotically correlates with the initial state) are practically the same as those obtained by including additional  $\phi_i$  states. As a consequence, for the collision processes investigated here, the resonances can be considered as isolated.

More important is to study the convergence with respect to the number of continuum states included in the expansions. In Fig. 2 we have plotted the transition probabilities versus impact parameter for  $v=0.006$  a.u., obtained with an increasing number of continuum states. In all cases, only

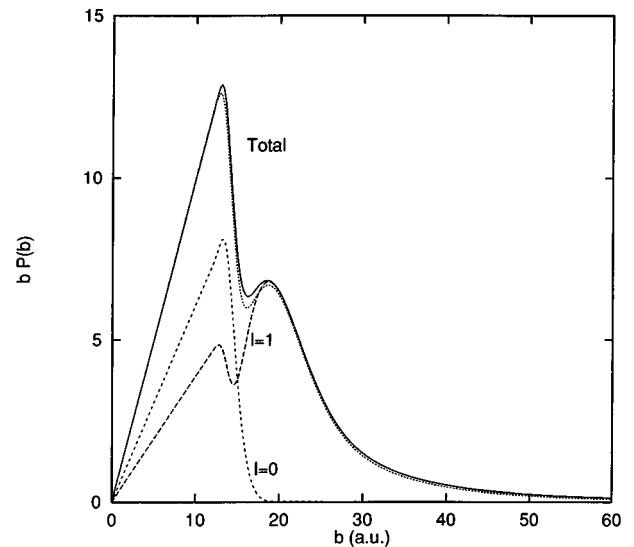


FIG. 3. Contribution of the  $l=0$  and 1 components to the converged Penning detachment transition probability shown in Fig. 2. The dotted line shows the results of the local approximation.

$l=0$  and 1 angular momenta have been included in the continuum. Convergence is achieved when the energy separation between neighboring continuum states is rather small. The continuum states that are significantly populated at a given time  $t$  are those that lie in a region of width  $\Gamma(t)$  around the resonance  $\phi_0$ . Consequently, if one tries to work with too small a number of continuum states near the resonance, one could obtain cross sections very much in error. Since the position of  $\phi_0$ ,  $E_0(t)$ , is a function of  $t$ , a fine energy spacing must be used throughout the whole energy interval in which  $E_0(t)$  varies. In contrast there is no need to use such a fine energy spacing away from the resonance (in fact, the upper cutoff used in this convergence study could have been much lower).

Due to the long-range nature of the Penning detachment process (see above and [1]), one can expect that the dipole-dipole term of the multipolar expansion of  $1/r_{12}$  is responsible for most of the relevant couplings of the process. Since the ejected electron initially occupies the  $1s$  orbital of  $H^-$ , the consequence is that most of the electrons must be ejected into continuum orbitals with  $l=1$ . This conjecture is supported by our calculations: the converged total ionization probability obtained by including  $l=0$  and 1 continuum states barely differs from that obtained by including  $l=1$  only. Looking at the  $l=0$  and  $l=1$  contributions separately (Fig. 3), we observe that the most important effect of the  $l=0$  continuum states is to absorb probability flux from the  $l=1$  states, which are directly populated from  $\phi_0$ . As argued in Sec. II B, this is done through the  $\langle \psi_{E, l} | P_l \mathcal{H}_{el} P_{l'} | \psi_{E', l'} \rangle$  couplings. However, direct transitions from  $\phi_0$  to the  $l=0$  continua are not very important. A similar effect can be expected if one includes continuum states with  $l>1$ . For this reason we have limited the sum in  $l$  [Eq. (8)] to  $l=0$  and 1 in all calculations.

It is interesting to compare the close-coupling results with the local approximation presented in Sec. II B because most of the hypotheses for the validity of this model are approximately fulfilled. For this purpose, we have evaluated the

resonance width  $\Gamma$  defined in Eq. (20) from the same coupling matrix elements used in the close-coupling calculations. Figure 3 shows the total transition probability versus impact parameter obtained with both the local approximation and the close-coupling method. As can be seen, the results are almost identical, which proves the validity of the local approximation to obtain Penning detachment cross sections in the present case. For the case of straight-line nuclear trajectories, computational effort is comparable in both cases because most of the time is spent in the evaluation of the coupling matrix elements. On the other hand, when trajectory effects are important, the solution of the system of coupled equations is more involved than the use of the local approximation. For this reason, the results obtained in Sec. IV by including the effect of the trajectory have been obtained within the local approximation.

#### IV. CROSS SECTIONS

We have calculated Penning detachment cross sections for collision energies between 25 meV and 20 eV ( $v_0 \approx 0.001-0.025$  a.u.) for the following cases: (i)  $\text{H}^- + \text{He}(1s2s, ^1S)$ , (ii)  $\text{H}^- + \text{Li}(1s^22p)$ , (iii)  $\text{H}^- + \text{Li}(1s^23s)$ , (iv)  $\text{H}^- + \text{Li}(1s^23p)$ , and (v)  $\text{H}^- + \text{Li}(1s^23d)$ . (Energies are expressed in laboratory frames, not in center-of-mass frames, since these are what is measured directly in typical experiments.) In cases (i) and (ii), the final states are  $\text{H} + \text{He}(1s^2) + e^-$  and  $\text{H} + \text{Li}(1s^22s) + e^-$ , respectively. In cases (iii)–(v) decay to  $\text{Li}(1s^22p)$  is also possible. One of the aims of the present section is to study the variation of the Penning detachment cross section with impact energy. One might expect cross sections to decrease with impact energy, but we will see that there are exceptions to this generalization. The energy range covered by the present calculations allows us to analyze the effects responsible for the various variations that occur with energy. Another point of interest is to study the dependence of the cross sections on the initial state of the neutral atom for a fixed final state of the neutral. Cases (iii)–(v) allow decay to several final states, which makes them very attractive for both experimental and further theoretical investigation. It should be possible to observe some of the possible final channels, such as  $\text{Li}(1s^22p)$ , via detection of the radiative decay of the residual excited state of Penning detachment. In all cases considered in these calculations thus far, however, the residual state of the energy donor, following detachment, is of  $S$  symmetry. This contribution can be determined from experiment, in cases (iii)–(v), by subtraction from the total detachment cross section of the contribution of any residual states that radiate down to the  $S$  state following detachment. Also, as the only effective couplings at the low energies considered in this work are those induced by the electronic Hamiltonian between  $P$  and  $Q$  subspaces (as explained in Sec. II, nonadiabatic dynamical couplings are negligible) and the final states have only  $m=0$  components, the largest cross sections for the non- $s$ -initial states will correspond to the  $m=0$  components. For this reason we will only consider detachment from initial  $m=0$  states.

According to the model of Blaney and Berry [1], in which the Penning detachment process can be interpreted as a dipolar deexcitation of the target with a simultaneous excita-

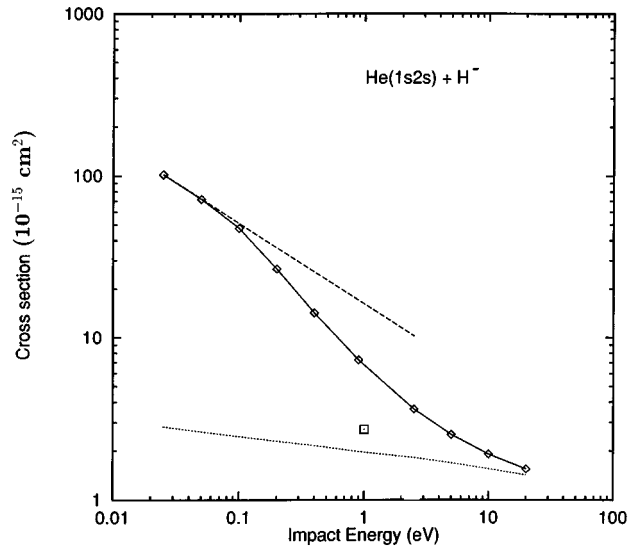


FIG. 4. Penning detachment cross section for the  $\text{H}^- + \text{He}(1s2s, ^1S)$  collision. Continuous line with diamonds, present results; dashed line, Langevin approximation; dotted line, results obtained by using straight-line trajectories; square, results from Blaney and Berry [1].

tion from the ground state of the anion to the continuum, Stark mixing is necessary in cases (i), (iii), and (v) in order to have significant Penning detachment cross sections. On the other hand, in cases (ii) and (iv) the excited electron is already in a  $p$  orbital, so that dipolar decay should be much more effective. Another important aspect that we are able to analyze by comparing He and Li targets is the role of the excitation energy of the neutral atom. Indeed, excitation energy in case (i) is much larger than in cases (ii)–(v) and therefore the mean kinetic energy of the ejected electrons must be larger. The results presented in this section will help to clarify these points.

##### A. $\text{H}^- + \text{He}(1s2s, ^1S) \rightarrow \text{H} + \text{He}(1s^2) + e^-$

Figure 4 shows the Penning detachment cross section for  $\text{H}^- + \text{He}(1s2s, ^1S)$ . In the same figure we have included the close-coupling results obtained using straight-line trajectories. As expected, the effect of the nuclear trajectory is small at higher energies where the cross section tend to the linear-trajectory results. However, at lower energies, the attractive nature of the interatomic potential [see Fig. 1(a)] makes the couplings much more effective than at high energies because the nuclei spend a much larger time close to each other. As a consequence, the transition probability increases. Such an effect is especially important at large impact parameters, for which the linear-trajectory calculations predict that transition probability is negligible. This is clearly illustrated in Fig. 5.

The origin of the attractive nature of the interatomic potential is the interaction of the  $\text{H}^-$  ion with the induced dipole of the neutral atom. Asymptotically, this potential is given by

$$V(R) = -\frac{\alpha}{2R^4}, \quad (35)$$

where  $\alpha$  is the polarizability of the excited  $^1S$  state of He.

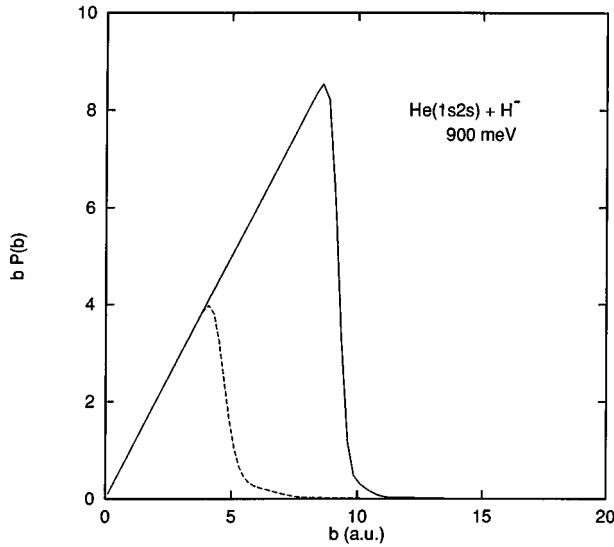


FIG. 5. Penning detachment transition probability times the impact parameter as a function of impact parameter for the  $H^- + \text{He}(1s2s, ^1S)$  collision at 900 meV. Continuous line, trajectory effects included; dashed line, results obtained by using straight-line trajectories. Only spin coupling  $S=1$  is shown.

Classical scattering of particles by this potential has been considered by Langevin [12] in the study of mobility and diffusion coefficients. He found that, for a given impact energy, the deflection angle increases systematically with decreasing impact parameter  $b$ , until a limit value  $b_0$  is reached, the Langevin radius, below which the impinging particle orbits into the target. The Langevin radius is related to the polarizability through the equation

$$b_0 = \left( \frac{4\alpha}{\mu v_0^2} \right)^{1/4}. \quad (36)$$

Then  $b_0$  increases when  $v_0$  decreases. At sufficiently low impact energy, transitions in the  $H^- + \text{He}(1s2s, ^1S)$  system take place at very long internuclear distances, where the interatomic potential is approximately given by Eq. (35). Therefore, for  $b < b_0$ , the  $H^-$  ion orbits about the He atom, so that there is enough time for the couplings to be effective. As a consequence,  $P_{\text{ion}}(b) \approx 1$  for  $b < b_0$  and the cross section becomes

$$\sigma_{\text{ion}} = \pi b_0^2. \quad (37)$$

We have evaluated the polarizability of the  $\text{He}(1s2s, ^1S)$  state by fitting the calculated potential-energy curve [Fig. 1(a)] to Eq. (35). The resulting value is  $\alpha = 534$  a.u. [13]. Using this value, we have evaluated the Langevin cross section from Eqs. (36) and (37). The corresponding results are also shown in Fig. 4. This figure shows that the actual cross section tends to the Langevin values at low energies. The Langevin cross section is almost two orders of magnitude larger than the one obtained with linear trajectories. Therefore, the variation with energy of the Penning detachment cross sections can be explained as a transition from a Langevin regime to a linear regime.

In Fig. 4 we have also included the cross section calculated at 1 eV by Blaney and Berry [1], who used straight-line

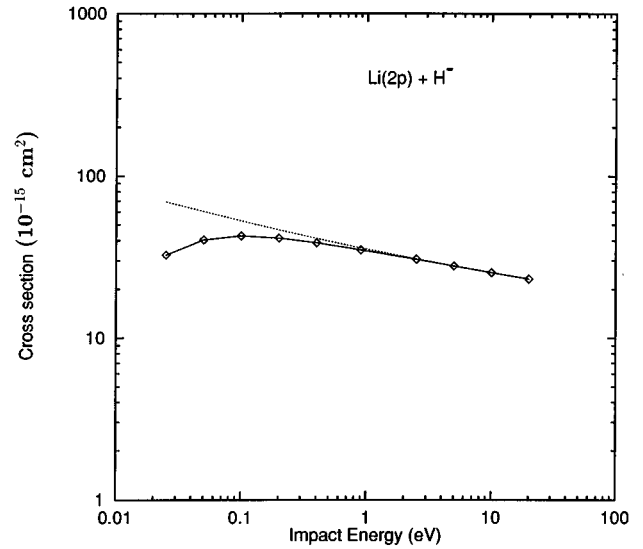


FIG. 6. Penning detachment cross section for the  $H^- + \text{Li}(1s^22p)$  collision. Continuous line with diamonds, present results; dotted line, results obtained by using straight-line trajectories.

trajectories and a very simple model to describe the Stark mixing. Their result is close to ours in the straight-line approximation, but it is significantly smaller than the one obtained by including trajectory effects. Therefore, the present results suggest that Penning detachment cross sections are even larger than anticipated by Blaney and Berry.

### B. $H^- + \text{Li}(1s^22p_0) \rightarrow \text{H} + \text{Li}(1s^22s) + e^-$

In Fig. 6 we present the values of the calculated cross section for  $H^- + \text{Li}(1s^22p_0)$ . In this case the straight-line approximation is very good approximation in most of the energy range investigated here. This can be understood with the help of Fig. 7, where we have plotted the transition probability versus impact parameter for 900 meV impact energy. Note that some transitions take place even at very long internuclear distances ( $R \approx 30$  a.u.), where the interatomic potential is almost flat, so that the nuclear trajectory is practically a straight line. At very low energies, however, the cross section decreases slightly with impact energy, which is due to the slightly repulsive character of the interatomic potential at long distances; in this case there is no attractive interaction between the  $H^-$  ion and the neutral atom because the latter is in a  $P$  state.

### C. $H^- + \text{Li}(1s^23s, 3p_0, 3d_0) \rightarrow \text{H} + \text{Li}(1s^22s) + e^-$

Figure 8 shows the Penning detachment cross section for  $H^- + \text{Li}(1s^23s)$ ,  $H^- + \text{Li}(1s^23p_0)$ , and  $H^- + \text{Li}(1s^23d_0)$ . In the same figure we have included the close-coupling results obtained using straight-line trajectories. The potential-energy curves associated with these three states are attractive in the region where the couplings are effective, so that the cross sections including trajectory effects are larger than those obtained in the straight-line approximation. As in Sec. IV A, the differences decrease with increasing energy and, for the higher energies, the two types of calculations lead to similar results. In the case of the  $\text{Li}(1s^23s)$  target, the inter-

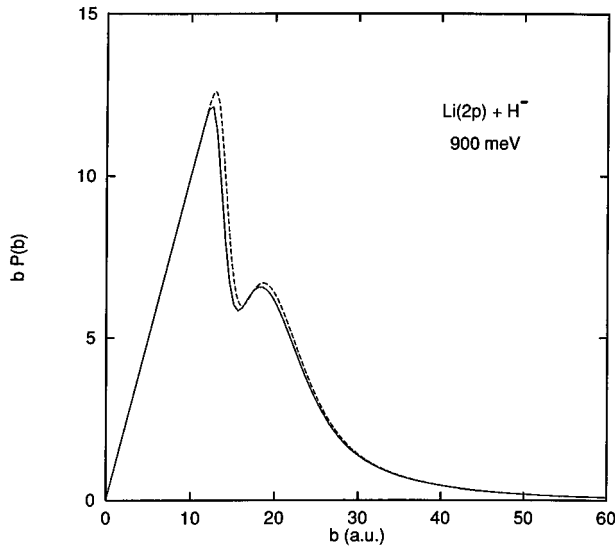


FIG. 7. Penning detachment transition probability times the impact parameter as a function of the impact parameter for the  $H^- + Li(1s^2 2p)$  collision at 900 meV. Continuous line, trajectory effects included; dashed line, results obtained by using straight-line trajectories. Only spin coupling  $S=0$  is shown.

atomic potential behaves as in Eq. (35) for large  $R$ , so that it is possible to evaluate the polarizability ( $\alpha=4262$  a.u.) and hence to obtain the Langevin cross section. The latter has also been included in Fig. 8. Since the polarizability is larger than for  $He(1s2s,^1S)$ , the Langevin cross section is also larger. As in Sec. IV A, the cross section tends to the Langevin cross section at very low energies, so that the same global behavior is observed. The Penning detachment cross section for  $Li(1s^2 3p_0)$  is comparable to the former in all the energy range, and so is that of  $Li(1s^2 3d_0)$  above 400 meV. This is a consequence of the strong Stark mixing between the neighboring  $3s$ ,  $3p$ , and  $3d$  orbitals of Li, so that having the

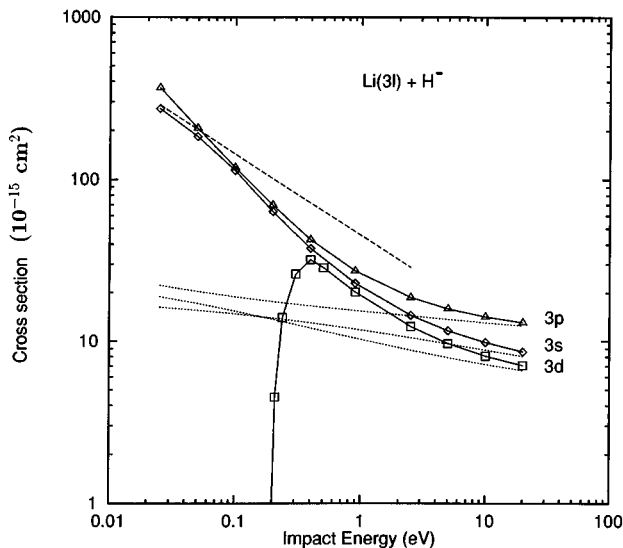


FIG. 8. Penning detachment cross section for the  $H^- + Li(1s^2 3s, 3p, 3d)$  collisions. Continuous lines, present results; dashed line, Langevin approximation; dotted lines, results obtained with straight-line trajectories.

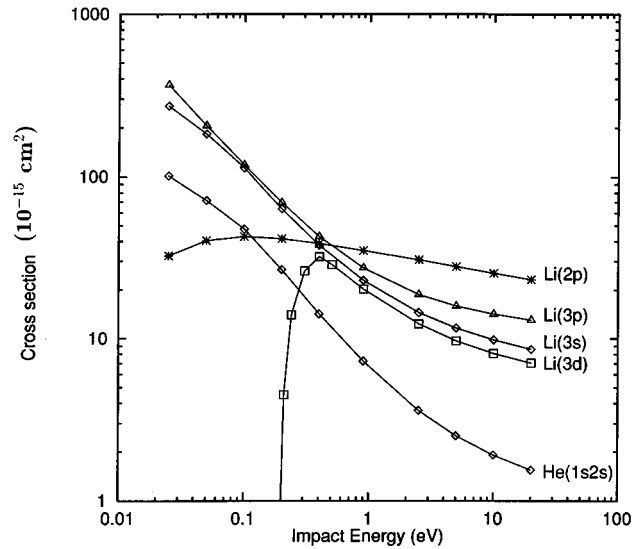


FIG. 9. Comparison between Penning detachment cross sections for the  $H^- + He(1s2s,^1S)$  and  $H^- + Li(1s^2 3s, 3p, 3d)$  collisions.

excited electron in a  $p$  orbital of the neutral atom in such cases does not produce larger Penning detachment cross sections. The behavior for  $Li(1s^2 3d_0)$  below 400 meV is striking. This cross section has a maximum at this energy and sharply decreases at lower energies; for  $E < 200$  meV it is practically zero. The reason for this behavior is the occurrence of a barrier in the interatomic potential at  $R \approx 22$  a.u. [see Fig. 1(b)]. This barrier is the result of an avoided crossing with the upper potential-energy curve, which dissociates into  $Li(1s^2 4s)$ . For  $E < 400$  meV, the barrier is high enough to prevent the  $H^-$  ion from going into the inner well of the potential. As a consequence, the couplings are no longer effective and the Penning detachment process shuts off at low collision velocities. This situation is not restricted to this state. It can be found for any repulsive state of a given Stark manifold that interacts with attractive states associated with higher manifolds.

#### D. Comparison between He and Li targets

It is interesting to compare the present results for Li and He. This comparison is made in Fig. 9. For  $E > 1$  eV, the cross section for Penning detachment for  $Li(1s^2 2p_0)$  targets is roughly an order of magnitude larger than for  $He(1s2s,^1S)$ . This is consistent with the crude model of Blaney and Berry: in the first case, dipolar decay is more favored than in the second, for which Stark mixing is needed. However, at very low energies, one can observe just the opposite. This *anomalous* behavior for  $Li(1s^2 2p_0)$  targets appears because the ion-atom interaction potential deviates sharply from Eq. (35) even at large distances, so the system does not follow Langevin trajectories. In other words, the attractive nature of the  $H^- + He(1s2s,^1S)$  interatomic potential leads to an increase of the cross section with respect to the straight-line results, whereas the  $H^- + Li(1s^2 2p_0)$  interatomic potential is almost flat in the region where transitions take place. A similar conclusion applies to comparisons of  $H^- + Li(1s^2 2p_0)$  with  $H^- + Li(1s^2 3s)$ ,  $H^- + Li(1s^2 3p_0)$ , and  $H^- + Li(1s^2 3d_0)$  (except for  $E < 400$  meV in the latter case).

It can also be observed in Fig. 9 that, although Penning detachment cross sections for  $H^- + He(1s2s, ^1S)$  and  $H^- + Li(1s^23s)$  behave qualitatively in the same way, the latter decreases slower with increasing collision energy than the former. At lower energies, the cross sections are identical to the Langevin cross sections, which decrease as  $1/v_0$ . However, this model is no longer valid at higher energies, where Stark mixing governs most of the physics of the problem. Stark mixing of the  $Li(1s^23s)$  state with the neighboring  $p$  state is much larger and takes place at much larger distances than for  $He(1s2s, ^1S)$ . As a consequence, the transition  $Li(1s^23s) \rightarrow Li(1s^22s)$  is much more probable than  $He(1s2s, ^1S) \rightarrow He(1s^2)$ , which explains the observed behavior.

## V. CONCLUSION

The present work is a theoretical attempt to obtain accurate cross sections for Penning detachment of negative ions by impact of excited neutral atoms. Our results confirm that this is a highly probable process, especially at very low impact energies. Although Penning detachment cross sections are very large for a wide range of impact velocities, the physics of the process at low and high energies is quite different. At low energies (say, less than 200 meV), the high values of the cross sections are due to the attractive interaction between the ion and a highly polarizable target. For neutral atoms in metastable  $S$  states, the calculated cross sections is almost identical to the Langevin cross section obtained from purely classical considerations. In other cases, however, the Penning detachment process can be suppressed at low energies by the occurrence of energy barriers in the interatomic potential. This is the case, for instance, of the  $Li(1s^23d)$  initial state.

At high energies (say larger than 1 eV), the dominant feature is the dipolar decay of the excited neutral atom and therefore the most favorable situation corresponds to neutral atoms in  $P$  states, which decay to the  $S$  ground state. However, dipolar decay from excited states with different symmetries is still possible if Stark mixing with  $P$  states is important. The closer the states, the larger the mixing (hence the cross section). As a rule of thumb, excited states with electrons occupying excited orbitals with high principal quantum number  $n$  are the best candidates to undergo Penning detachment at high energies.

Finally some comments are appropriate regarding the validity of the classical description used in this work to describe the nuclear motion. The transition probabilities in the semiclassical calculations are already so high that full quantum corrections would at most make small, quantitative changes and perhaps add some oscillations not shown in the semiclassical method [especially in the case of  $Li(1s^23d)$ , where tunneling effects may play some role]. However, nuclear quantum effects may be essential in the description of differential cross sections (differential in the nuclear deflection angle). Now that there is experimental evidence for Penning detachment [4], it becomes worthwhile to look for more refined effects that would only be revealed accurately in full quantum calculations.

## ACKNOWLEDGMENTS

This research was supported by a Grant from the National Science Foundation. F.M. would like to acknowledge the support of the Ministerio de Educación y Ciencia (Programa de Movilidad Temporal de Personal Funcionario, Docente e Investigador No. PR95-235) for a sabbatical leave at the University of Chicago.

- 
- [1] B. Blaney and R. S. Berry, *Phys. Rev. A* **3**, 1349 (1971).  
 [2] F. C. Fehsenfeld, D. Albritton, J. A. Burt and H. I. Schiff, *Can. J. Chem.* **47**, 1793 (1969).  
 [3] D. Doweck, J. C. Houver, J. Pommier, C. Richter, T. Royer, and N. Andersen, in *Proceedings of the XVIth International Conference on the Physics of Electronic and Atomic Collisions, New York, 1989*, AIP Conf. Proc. No. 205, edited by A. Dalgarno, R. S. Freund, M. S. Lubell, and T. B. Lucatorto (AIP, New York, 1990), p. 501.  
 [4] S. Darveau, R. Niedzieliv, B. Prutzman, Z. Herman, and R. S. Berry (unpublished).  
 [5] K. Katsuura, *J. Chem. Phys.* **42**, 3771 (1965).  
 [6] R. D. Taylor and J. B. Delos, *Proc. R. Soc. London Ser. A* **379**, 179 (1982).  
 [7] Y. D. Wang, C. D. Lin, N. Toshima, and Z. Chen, *Phys. Rev. A* **52**, 2852 (1995).  
 [8] H. Bachau, P. Galan, F. Martín, A. Riera, and M. Yáñez, *At. Data Nucl. Data Tables* **44**, 305 (1990).  
 [9] A. Macías, F. Martín, A. Riera, and M. Yáñez, *Phys. Rev. A* **36**, 4179 (1987).  
 [10] C. C. Pekeris, *Phys. Rev.* **126**, 1470 (1962).  
 [11] Following common usage, we call Stark mixing any mixing of states that arises from an external electric field.  
 [12] P. Langevin, *Ann. Chim. Phys.* **5**, 245 (1905); E. W. McDaniel, *Collision Phenomena in Ionized Gases* (Wiley, New York, 1964).  
 [13] Since our one-electron description of He cannot distinguish between singlet and triplet symmetries, this value of the polarizability lies between the actual ones for the  $2^1S$  state ( $\alpha=800$  a.u.) and the  $2^3S$  state ( $\alpha=315$  a.u.); see M. Rerat *et al.*, *Phys. Rev. A* **48**, 161 (1993).